Astron. Astrophys. 324, 597–605 (1997)

ASTRONOMY
AND
ASTROPHYSICS

Continuum IR emission of Be star wind-compressed discs

John M. Porter

Astrophysics, School of Electrical Engineering, Electronics and Physics, Liverpool John Moores University, Byrom Street, Liverpool L3 3AF, UK

Received 20 November 1996 / Accepted 14 January 1997

Abstract. A prescription for the density of a wind compressed disc (WCD) is given and the IR emission of the disc is calculated. The prescription enables emission from WCDs to be calculated simply without recourse to full $2\frac{1}{2}$-dimensional ($2\frac{1}{2}$-D) modelling of rotating radiatively driven winds. It is shown that the standard WCD model is incapable of representing observed Be star discs.

As a guide for future research, various addenda to the WCD model are considered: internal density structure of the disc, decoupling of the matter and radiation fields in the wind and finally magnetic fields. Of these, it is only a magnetic field which may be sufficient as a suffix to bring the WCD model into line with observations. The magnetic field strength must be tens of gauss to begin to reproduce observations.

Key words: stars: emission-line, Be – stars: circumstellar matter – stars: mass loss – infrared: stars

1. Introduction

In common with other hot stars, Be stars are thought to possess fast radiatively-driven winds which are described well by current theory (Castor, Abbott & Klein 1975, Friend & Abbott 1986, Kudritzki et al. 1989). A Be star also has a dense disc in its equatorial plane (Waters 1986, Quirrenbach et al. 1994). A large problem in Be star research is to understand how these two such disparate regions (fast, polar wind, and dense, equatorial disc) may co-exist around one star. A factor which discriminates Be stars from "normal" B stars is that Be stars are fast rotators, and although they do *not* rotate at their break-up velocity (Slettebak 1979), the majority of them have been found to rotate at ~ 0.7 of their break-up velocity (Porter 1996). Rapid rotation therefore may be a significant ingredient to the generation of the two different circumstellar regions.

The dense equatorial disc emits free-free radiation in the IR and radio creating an excess over the photospheric emission which has been modelled phenomenologically by a variety of disc/slab models (Poeckert & Marlborough 1978, Waters 1986, Kastner & Mazzali 1989). Although these models have been successful in describing many elements of the energy distribution, the physical reason for the disc's existence and geometry has not been emphasized.

A variety of theoretical models has been proposed to explain the existence of the two regions. These include magnetic winds (Poe & Friend 1986), latitudinal variation of driving lines (de Araujo & de Freitas Pacheco 1989) and stellar pulsation (Willson 1986, Ando 1986) although the wind-compressed disc model (WCD) of Bjorkman & Cassinelli (1993) has attracted most attention recently. This model shows that under the influence of rotation, the radiatively-driven gas streamlines may be deflected towards the equatorial plane. As the deflected flows from both hemispheres collide at the equatorial plane, a dense shocked region forms - the wind-compressed disc. The mechanism has been shown to be correct in numerical hydrodynamic simulations of Owocki, Cranmer & Blondin (1994), although the properties of the disc in the numerical simulations differ widely from those predicted by Bjorkman & Cassinelli. One feature of the hydrodynamic simulations of Owocki et al. is that the disc has a much lower equator to pole density ratio than that predicted by Bjorkman & Cassinelli, which leads to much weaker IR emission from the WCDs than is observed in real discs.

Even though the simple WCD paradigm does not provide discs which could account for the observations, such an attractive model for the generation of an equatorial disc from the fast polar wind (and thereby differentiating B and Be stars by rotation) should be persued further. Here the IR emission of WCD models is calculated and compared with the emission of observed discs. With such a tool, a study can be made of the most important factors which could affect the emission of the disc. As the aim of this investigation is to assess whether the WCD model may be a viable theory for observed Be star discs then a consistency of WCD-emission to observed-disc emission to within of factors of a few is sufficient to assess if WCDs are reasonable representations; no individual star shall be concentrated upon, nor shall a "best-fit" model be produced. An investigation of the sort of low density discs found by Owocki et al. has already been undertaken by Zaal et al. (1995) and has shown that the IR emission of these discs is too small by orders of magnitude to be a good representation of Be star discs, although the standard

WCD theory may account for some stars with low density discs. By examining different properties of the polar wind and disc, light may be shed on any effect which is likely to be important in generating the sort of discs which have been observed. In short, the task undertaken here is to find how the WCD model may be supplemented to make the WCD a good representation of observed discs.

The rest of this paper is organised as follows: in Sect. 2 a prescription for the density structure of a WCD is presented. In Sect. 3 the IR emission from the model is calculated, and in Sect. 4 further developments to the WCD model are considered. Implications of this investigation are presented in Sect. 5.

2. Wind compressed disc model

To calculate the IR emission of the circumstellar material around the central star, a density prescription for the equatorial disc needs to be specified. Here the density in the WCD is calculated by assuming pressure balance between the wind confining either side of the disc and the internal thermal pressure of the disc.

Necessarily, the model below is an approximation; the full solution of the time dependent fluid equations should be solved in at least $2\frac{1}{2}$-D in order to derive an "exact" density structure. However, this amounts to quite an undertaking, and the accuracy of the prescription below is sufficient to highlight the essential physics of the flow.

2.1. Wind structure

The velocity and density of the wind compressing the disc are calculated from Bjorkman & Cassinelli's (1993) prescription with the extension proposed by Owocki et al. (1994) to align the analytic model with numerical simulations (Owocki et al.'s section 4.3). This model uses Friend & Abbott's (1986) numerical solution for rotating radiation driven winds. They presented relationships between the mass-loss rate and rotational velocity, and the terminal velocity of the flow and the rotational velocity. These relationships can then be used to calculate the velocity and density in a streamline, given a foot-point for the streamline on the star.

The wind velocity and density structure are assumed to have little effect on the IR emission (see Sect. 3), and so it is calculated only to enable the compression-disc structure to be derived.

2.2. Disc density and structure

In the general case, the disc will not have a constant opening angle, and so the geometry of the disc will be as shown in Fig. 1. With components of the velocity of the wind in the r and θ directions as v_r and v_θ, the total external wind pressure P_e exerted on the disc is the sum of ram pressure P_n normal to the disc's surface, and thermal pressure P_t:

$$P_e = P_n + P_t =$$

$$\rho_w \left\{ (v_r^2 + v_\theta^2)\sin^2\left[\psi - \theta + \arctan\left(\frac{v_\theta}{v_r}\right)\right] + a_w^2 \right\}, \qquad (1)$$

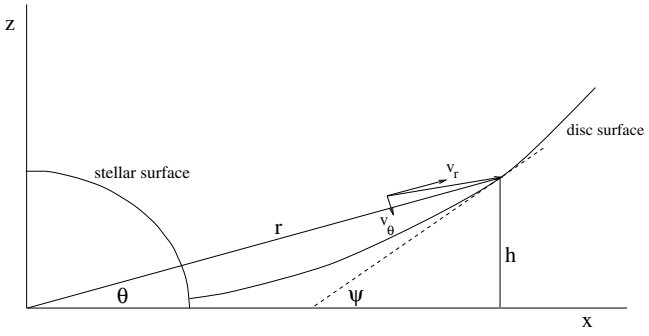

Fig. 1. Geometry of the WCD

where θ and ψ are shown in Fig. 1, a_w is the sound speed in the wind, and ρ_w is the wind density.

This external pressure is matched by the internal gas pressure in the disc $P_d = \rho_d a_d^2$ where ρ_d is the disc density, and a_d is the sound speed in the disc. Equating these two expressions for a disc in pressure balance, the disc density is

$$\rho_d = \rho_w \left\{ \left(\frac{v_r^2 + v_\theta^2}{a_d^2}\right) \sin^2\left[\psi - \theta + \arctan\left(\frac{v_\theta}{v_r}\right)\right] + \left(\frac{a_w}{a_d}\right)^2 \right\}. \qquad (2)$$

For the special case of a disc with a constant opening angle ($\theta = \theta_{\rm op} = \psi$ =constant) this reduces to

$$\rho_d = \rho_w \left\{ \left(\frac{v_r^2 + v_\theta^2}{a_d^2}\right) \mathrm{s}\left[\arctan\left(\frac{\mathrm{v}_\theta}{\mathrm{v}_\mathrm{r}}\right)\right] \mathrm{in}^2 + \left(\frac{a_w}{a_d}\right)^2 \right\}$$

$$= \rho_w \left\{ \frac{v_\theta^2 + a_w^2}{a_d^2} \right\}. \qquad (3)$$

Note that this expression for ρ_d is explicitly independent of the opening angle $\theta_{\rm op}$, although it depends on $\theta_{\rm op}$ via the wind velocity and density at which a particular streamline intersects with the disc. The variation of v_θ may be large near $\theta = 90°$ (see Owocki et al.'s Fig. 5c) and so the disc density may change significantly. However, for $\theta_{\rm op} \sim 5° \rightarrow 10°$, the disc density variation leads to a maximum difference in the IR emission of the models of around 2 (see Sect. 3 later). As this study is very much a feasibility study of the emission from such discs, the exact choice of $\theta_{\rm op}$ in the range 2°-10° is not very important. Also, as the assumption of a constant opening angled disc simplifies the problem somewhat, then the approximation is used (note also that in Owocki et al.'s calculation the opening angle of the disc does not vary over a large range for each model).

The disc will now be split into two regimes: the *inner disc* and *outer disc*. The inner disc is defined where the velocity of the wind normal to the disc (leading to the compressive force) is greater than the sound speed ie. the Mach number of the wind normal to the disc's surface is greater than unity: here the disc is actively compressed by the wind. The inner disc is assumed to

have a constant opening angle. Although the outer disc's local opening angle ψ may be calculated consistently (see below), in practice the outer disc has a nearly constant opening angle also (see Sect. 2.2.2).

The compression ratio $\mathscr{C}$ is now introduced for a disc of constant opening angle, and is defined as the ratio of the compression due to the wind streamline motion (through v_θ) and the thermal compression from the wind (through the wind's sound speed):

$$\mathscr{C} = \left(\frac{v_r^2 + v_\theta^2}{a_w^2}\right) \sin^2\left[\arctan\left(\frac{v_\theta}{v_r}\right)\right] = \frac{v_\theta^2}{a_w^2}. \quad (4)$$

The position of the boundary (x_b) between the inner and outer discs is defined when $\mathscr{C} = 1$. As x increases v_r increases and v_θ decreases and so the sine term in $\mathscr{C}$ decreases quickly. This is because the streamlines after being initially deflected toward the equator, quickly become radial (see Fig. 5 of Bjorkman & Cassinelli) and so the compressive force on the discs drops rapidly. It should be noted that the compression ratio $\mathscr{C}$ drops below unity for radii very close to the stellar radius. This is in the region in which the disc be being constrained by streamlines having foot-points very close to the equatorial plane. These streamlines are deflected little to the equatorial plane as their flow direction is essentially parallel to the disc anyway.

2.2.1. Inner disc

In this regime the disc is assumed to have a constant opening angle with a nominal value of $\theta_{\rm op} = 5°$. Note that with the assumption of constant opening angle, the velocity of the outflowing gas in the disc may also, in principle, be calculated from the mass conservation equation

$$\frac{d}{dr}(\rho_d v_d r h) = \rho_w v_n r, \quad (5)$$

where $h = x\tan(\theta_{\rm op})$ is the disc height at distance x from the star and v_n is the velocity of the wind normal to the disc's surface. This is not attempted here for two reasons: (i) if the assumed constant opening angle $\theta_{\rm op}$ is varied, it has little effect on the IR emission (from 5°-10°) but it has a large effect on the disc's velocity: the smaller $\theta_{\rm op}$ is, the larger the velocities will be to keep the same mass flux within the disc (and vice-versa), and (ii) a boundary condition needs to be specified to solve Eq. 5. This is not trivial: Owocki et al. (1994) found re-accretion of wind material, suggesting that the simple condition $v_d = 0$ at $x = R_\star$ will be likely to be incorrect for most (if not all) models. Without solving the momentum equation within the disc and hence doing a $2\frac{1}{2}$-D or 3-D numerical solution of the flow (something out of the realm of this paper) calculation of the velocity of the disc is not attempted. This cautious approach to the disc velocity field is necessary so that over-interpretation of the current model's dynamics is avoided.

2.2.2. Outer disc

In the outer portions of the disc, the compressive force due to the wind streamlines drifting toward the equator is less than the thermal pressure in the wind. In this case, the gas in the disc is not being "squeezed" and the outward velocity of the gas in the disc will remain approximately constant at the terminal velocity v_t^d. Also, the wind only *confines* the disc from x_b outwards (there is be a negligible mass flux input to the disc) and so the mass flux in the disc can be assumed to be constant. From mass conservation at the boundary between the discs,

$$x h \rho_d = \frac{\dot{M}}{2\pi v_t^d} = \text{constant}, \quad (6)$$

where h is the value of the disc height (note that at the boundary $h = x\tan(\theta_{\rm op})$).

Combining this with Eq. 2, and after some manipulation the value for the the angle to the horizontal of the local tangent ψ is given by

$$\sin(\psi - \theta) = \left\{\left[\frac{\dot{M}}{2\pi v_t}\right]\frac{a_d^2}{x h \rho_w v_r^2} - \left(\frac{a_w}{a_d}\right)^2\right\}^{\frac{1}{2}}, \; x > x_b \quad (7)$$

where v_θ has been assumed to be small compared with v_r. The assumptions made above ensure that the term in square brackets above is a constant and may be evaluated at the boundary point x_b using Eq. 6. The height of the disc is then a simple integral

$$h(x) = \int_{x_b}^{x} \tan\psi \; dx \; + \; h_c \quad (8)$$

which can be solved simultaneously with Eq. 7 to obtain the height of the disc. The disc density can then be calculated using Eq. 6 as, again, the value of $\dot{M}/2\pi v_t$ is constant, leaving the density simply depending on this constant divided by the height of the disc and x. The local opening angle ψ changes little from $\theta_{\rm op}$ in the outer disc. This is because at these large radii v_r has risen to a value close to the terminal wind velocity, and hence from Eq. 6, $\rho_d \propto 1/xh$, and through mass conservation in the wind $\rho_w \propto 1/r^2 = 1/x^2$ in the equatorial plane. These combine to ensure that the first term on the RHS of Eq. 7 is approximately constant. Also, for an isothermal model the second term is constant, and so the opening angle becomes approximately constant, leading to the disc density falling off as x^{-2}.

2.2.3. Example calculation

As an example of the model describe above and also to examine the assumptions, the WCD structure is calculated for the same model B2 star as was considered by Owocki et al. (1994) in their numeric calculations. The stellar parameters for this star are $M_\star$ = 7.5$M_\odot$, $L_\star$= 2310$L_\odot$, $R_\star$ = 4$R_\odot$and T$_*$ = 20,000K. This model star has a critical rotation velocity of 488km s^{-1}, and (for direct comparison with the model Owocki et al. present in most detail) rotates at 0.7 of its break-up velocity (350km s^{-1}). An isothermal model is used such that the wind sound-speed is the same as the disc sound-speed $a_w = a_d$. Constant opening angles of 2°, 5°, 10°, are used, (Owocki et al. find an opening angle of $\sim$ 2°). The model is calculated as follows: the wind

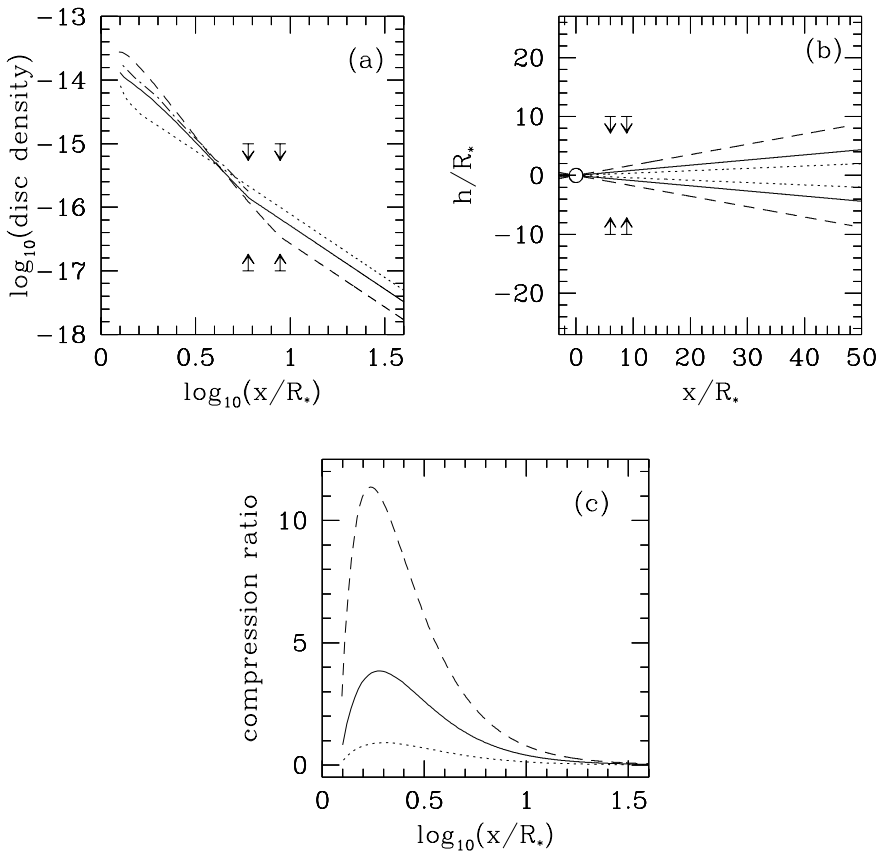

Fig. 2a–c. The WCD model for three opening angles: 2° (dotted line), 5° (solid line), 10° (dashed line). **a** disc density (in g cm^{-3}) as a function of radius (the dot-dash line is the density from Owocki et al.'s simulation with an outer radius of $6R_\star$): **b** the disc shape: **c** the compression ratio versus radius (see text). For **a** and **b** the arrows indicate the boundary between the inner and outer disc for the 5° and 10° discs (compare with **c** at a compression ratio of unity).

streamlines are determined first, and those which cross the inner disc boundary at $\theta = \theta_{\rm op}$ are flagged and the inner disc density is calculated. For the outer disc, the height of the disc is calculated from Eq. 7 and Eq. 8 and then the density is calculated. As the streamlines are typically nearly radial when they intersect the disc at large distances from the star, then typically 500 different streamlines with foot-points equally spaced in θ on the star are used. The streamlines are calculated to a radius of $50R_\star$ if they do not intersect the disc.

Fig. 2a and b display the disc density and disc shape for the model star for the three opening angles. Also in Fig. 2a the density profile from Owocki et al.'s simulation is included (the dot-dashed line – their simulation's outer radius was $6R_\star$). The arrows indicate where the compression ratio falls below unity. The arrow closer to the star is for the calculation with $\theta_{\rm op} = 5°$ at $5.8R_\star$, and the other is for $\theta_{\rm op} = 10°$ at $8.7R_\star$. The model with $\theta_{\rm op} = 2°$ has a compression ratio always less than unity. Fig. 2c shows the compression ratio $\mathscr{C}$ for the models: the boundary between inner and outer disc occurs when this ratio falls to unity. The parameters derived from the model above with $\theta_{\rm op} = 5°$ and those given by Owocki et al. typically agree to within a factor of two.

3. IR continuum emission from the WCD

Now that the WCD has been specified, its IR continuum emission may be calculated. For simplicity, the star is assumed to be pole on and the prescription used for the calculation is that given by Waters (1986). The emission comes from the free-free emission from the hot plasma in the disc. The contribution from the wind is not significant and so it is disregarded and the emission is calculated solely from the disc. The underlying photospheric emission from the star is assumed to be a black-body: again, this is an accurate enough assumption to be able to make statements concerning the mechanism for creating the disc.

In order to assess the applicability of the model, the emission from a constant opening angle disc model has been calculated. This disc has an opening angle of 15°, a density law $\rho = \rho_0(r/R_\star)^{-2.5}$ with $\log(\rho_0/{\rm gcm}^{-3}) = -11.5$ which are typical values used to fit IR observations of Be stars (Waters 1986, Waters, Coté & Lamers 1987). The calculation was stopped at an outer radius of $100R_\star$.

Fig. 3a shows the IR continuum emission for the model above with the three values of opening angle $\theta_{\rm op} = 2°,\ 5°,\ 10°$ all with the central star rotating at 0.7 of the break-up velocity. Given in Fig. 3b are the spectra given by the model for different rotation rates (0.5, 0.7 and 0.9 of the break-up velocity). As the distribution of rotation velocity as a fraction of break-up is sharply peaked at around 0.7 (see Porter 1996), and statistically the opening angle defined in this way of shell stars is $\sim 5°$ (Porter 1996, Hanuschik 1996?), a disc with a 5° opening angle with an underlying star rotating at 0.7 of its break-up velocity will adopted hereafter as the standard model parameters for the WCD throughout the rest of this work.

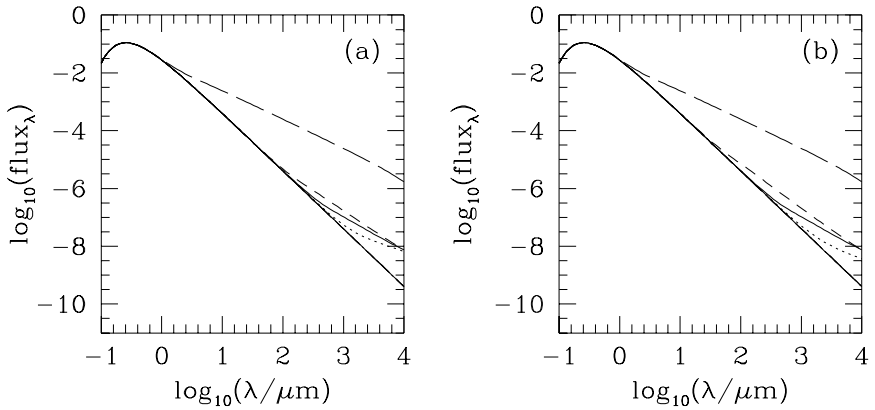

Fig. 3a and b. IR continuum emission form the standard WCD model: **a** emission from a WCD and star rotating at 0.7 of its critical (break-up) velocity $v_{\rm crit}$ with opening angles 2° (dotted line), 5° (solid line), 10° (short dashed line). The long dashed line is the emission from the disc model of Waters (see text). **b** emission from stars with an inner disc with an opening angle of 5° rotating at $0.5v_{\rm crit}$ (dotted line), $0.7v_{\rm crit}$ (solid line), $0.9v_{\rm crit}$ (short dashed line); again the disc model is the long dashed line. All of the spectra have been normalised, and black-body is used for the underlying stellar photospheric emission.

The magnitude of IR emission from a disc is determined by the temperature of the disc, its density, and how fast the density falls off with radius (see Waters 1986 Sect. 4.3). As the temperature is regarded as constant for the different models here, the variation in emission is dominated by the density within the disc. With a constant opening angle for all models for the inner disc, Eq. 3 shows that the ratio of v_θ/v_r will then define the IR emission. Hence a model which results in v_θ/v_r being (in)significant compared with unity will lead to a (small) large excess emission. Therefore the generation of emission similar to that observed must (i) have v_θ/v_r reasonably large compared with unity at the inner portions of the disc, and (ii) have v_θ/v_r decline slowly with increasing radius. This will then force the boundary between the inner and outer portions of the disc to a larger radius.

As can be seen from Fig. 3 the emission is woefully inadequate (by orders of magnitude) for the WCD to be a plausible description on its own of the circumstellar matter around of Be stars. This is illustrated by the fact that the boundary between inner and outer discs is close to the star. Hence, it seems that the WCD model in it's simplest form is not a complete description of Be star discs. However, it is premature to dismiss the WCD model at this juncture: this is the only self-consistent model of disc formation yet presented, and is a natural result of rotating winds. As it is highly attractive, the model is persevered with in order to assess if discs generated in this way *can* be responsible for the IR emission of Be stars.

4. Simple addenda to the WCD model

Clearly the previous section illustrates that the WCD model in its simplest form is not responsible for the excess IR emission from Be stars. However, it is now possible to investigate other effects which may be important. Some of the points discussed below have little *a priori* justification. However, their discussion may point future investigations toward the most likely cause for the generation of discs capable of reproducing the observations.

4.1. Internal structure in the disc

In the analysis above the density in the disc is assumed to be constant at a given distance from the centre of the star: this assumption is now relaxed. No explanation is sought for this variation: it is investigated simply to assess if it may be an important factor.

The density derived above in Eq. 2 for the compressing wind is now identified as the immediate postshock density. Can the disc density increase from the surface of the disc to the equatorial plane and hence increase the IR emission? A simple limit may be placed on the density contrast that may be maintained. The density at the surface of the (ie. the postshock density) disc is ρ, and the density at the centre of the disc (on the equatorial plane) has a density of $\rho + \Delta\rho$. The time taken for a pressure wave to travel in the z direction across the disc is $t_z \sim h/a_d$. This is typically the timescale over which the disc will come into pressure equilibrium with itself, and hence smooth out the density variation $\Delta\rho$. For the centre of the disc, the relevant timescale is that taken for the density of a parcel of gas to drop from $\rho + \Delta\rho$ to ρ caused by the radial flow (at velocity v_d) in the x direction of the disc. This is $t_x \sim \Delta\rho/(v_d|d\rho/dx|)$.

Hence, the density variation $\Delta\rho$ can only be maintained if the horizontal flow timescale in the disc t_x is less than the time taken for the disc to come into pressure equilibrium t_z. Therefore the maximum density variation will be generated when these timescales are equal $t_x = t_z$ or

$$\frac{h}{a_d} = \frac{\Delta\rho}{\left|\frac{d\rho}{dx}\right|}\frac{1}{v_d}. \tag{9}$$

The results of the WCD model in Sect. 2 yield that the density in the disc (at least over some range of x) is similar to a power law $\rho = \rho_0(r/R_\star)^{-n}$, where ρ_0 is the disc density at the $r = R_\star$. For illustration, this is now assumed and Eq. 9 becomes

$$\frac{\Delta\rho}{\rho} = n\frac{h}{x}\frac{v_d}{a_d}. \tag{10}$$

For a disc with a constant opening angle $\theta_{\rm op} = 5°$, $h/x = \tan(\theta_{\rm op}) = 0.09$ and with $n \approx 2.5$, (eg. Waters 1986)

$$\frac{\Delta\rho}{\rho} = 0.2\frac{v_d}{a_d}. \tag{11}$$

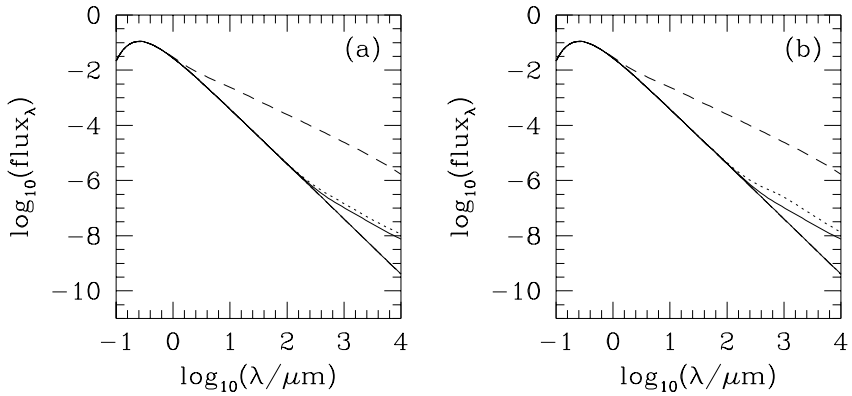

Fig. 4. a Emission from the standard WCD model with the star rotating at 0.7 of its break-up velocity with opening angle of 5° (solid line), a WCD with internal density structure from Eq. 11 (dotted line). The long dashed line is the emission from the disc model of Waters (see text). **b** emission from the standard WCD model with the star rotating at 0.7 of its break-up velocity with an opening angle of 5° (solid line), a WCD with matter-radiation field decoupling at $1.2R_\star$ (dotted line). Again the disc model is the long dashed line.

The velocity in the disc v_d is likely to not exceed $\sim 10^2 \text{km s}^{-1}$(at least for the regions in which Hα is formed, Waters & Marlborough 1992) and so $\Delta\rho/\rho \sim 2$. This is typically the maximum density contrast which may be supported by a flowing disc.

For the standard model a variation of $\Delta\rho/\rho = 2$ with a linear increase with z of the density from the disc surface to the equatorial plane is used to revise the IR emission. This has the effect that the integrated density of the disc is a factor of 3/2 greater than before, and so the integral of the density squared (proportional to the optical depth through the disc) increases by 9/4. The effect of this is shown in Fig. 4a. It is clear that in this model the variation of the density is insufficient to explain the IR emission. Indeed the density contrast needs to be at least $\Delta\rho/\rho > 100$ to reproduce the observed emissions. However, this would imply that the centre of the disc would have to have a radial velocity of five hundred times the sound speed! This is clearly ruled out by the observations and so any density contrast in the disc is *not* responsible for the extra emission.

4.2. Wind decoupling

It has been shown elsewhere (Porter & Drew 1995, Springman & Pauldrach 1992) that the winds of B stars are prone to a dynamic decoupling between the radiation field and the gas flow. This process may occur via two different mechanisms. The first is ion stripping, whereby the heavy elements in the flow which mediate the radiation force (eg. C, Si, N) are accelerated through the rest of the plasma at some radius – the decoupling radius – as the wind is not dense enough to be able to retard the ions due to the frictional force becoming too ineffective. Beyond this radius the wind essentially coasts, and is subject to no further radiative acceleration, ie. the gas flow has decoupled from the radiation field.

The second method by which decoupling may occur, is again due the low wind mass loss rate in B stars leading to low flow densities. The unstable nature of radiatively driven flows will naturally lead to shocks forming in the wind (Lucy & Solomon 1970, MacGregor et al. 1979, Owocki & Rybicki 1984, Owocki, Castor & Rybicki 1988). These shocks locally superionize the gas flowing through them. Radiation driving may only resume after a shock if the postshock gas regains its preshock ionization state. However, in the low density winds of B stars, it is possible that the number density is so low that this recombination is not possible. This leaves the postshock gas in a high ionization state, which does not have the same (or indeed any) of the resonance lines that the preshocked gas had, and hence radiative acceleration cannot resume decoupling the gas and radiation fields.

These two physical effects ensure that the wind receives no further acceleration and therefore the radial velocity remains approximately constant. Typically, decoupling radii may occur close to the star ($r_{\text{dec}} \approx 1.2R_\star$) (Porter & Drew 1995). Porter & Drew also demonstrated that such decoupling enabled a rotating wind to be more severely deflected toward the equator. As this mechanism has been shown to increase the momentum input normal to the disc, then it is included in the model for the IR emission. With the decoupling radius is set to $1.2R_\star$ the boundary between the inner and outer disc (where $\mathscr{C} = 1$), increases from $6R_\star$ (for the standard model) to $9.5R_\star$. The differences in the resultant IR emission are shown in Fig. 4b. Although this has increased the density by a factor of a few, and the IR emission by a similar amount, it is still unable to provide a complete explanation of the Be star disc.

4.3. Magnetic fields

Until now, the dynamics of the wind has been determined completely by the radiation force and rotational effects. As these have failed to produce circumstellar geometries that are implied by the observations, another mechanism that may introduce asymmetries into the wind must be considered. An obvious candidate here is a magnetic field. The effects of magnetism on radiatively-driven winds has already been considered by Friend & MacGregor (1984), Poe & Friend (1986), although these authors assumed that there were no meridional motions in the wind, and considered a magnetic field with only radial and toroidal components $\mathbf{B} = (B_r, 0, B_\phi)$.

Observational determination of the magnitude of Be star magnetic fields is difficult, as the effects of rotation blur out any Zeeman splitting in the atmospheric lines. However, some order of magnitude estimates are available: Nerney (1980) finds upper limits of 10G for Be stars, Barker et al. (1981), and also Landstreet (1982) find hot star magnetic fields to be undetectable over their errors of 100-200G, although they do point out that some

geometries of fields with kilogauss strength may not be detected in their work. Fox (1993) finds that the observed polarization of Be stars could be generated if the star has a magnetic field of $\mathbf{B} \lesssim 100$G. In their theoretical studies, Friend & MacGregor and Poe & Friend use magnetic strengths of upto 1600G. With this uncertainty in the magnetic field strength, a upper limit of tens of gauss seems reasonable.

Here the effect of a magnetic field on the meridional motions is considered in a non-rigorous fashion – the essence of the investigation is to establish the most probable mechanism for the Be star phenomena.

The WCD model is supplemented by the addition of a dipole field **B** aligned with the rotation axis. The streamlines are assumed to follow the magnetic field lines in the magnetically dominated regime where the magnetic energy density $|\mathbf{B}|^2/8\pi$ is greater than the wind's kinetic energy density $\frac{1}{2}\rho|\mathbf{v}|^2$, where **v** is the velocity of the wind. In this regime, the radial component of velocity is assumed to follow a β velocity law, as in the non-magnetic model – note that this is what was found in the radial/poloidal field in Friend & MacGregor, and Poe & Friend's work although the terminal velocities were different from non-magnetic models. The assumption of the β velocity law is incorrect as the retarding effect of the magnetic field in the radial direction has been ignored. However, this will lead to the magnetically-dominated regime being smaller in radial extent, as the kinetic energy density increases at least as fast as in the non-magnetic case.

Once the kinetic energy density is equal to the magnetic energy density then the magnetic field lines are pulled out of shape by the flow, and will follow the wind streamlines. In this regime, the streamline calculation is done exactly as before, except that the meridional velocity v_θ will only change if rotational effects cause it to increase beyond the value it has as the wind moves into the kinetic regime. The net effect of the magnetic field is to "slingshot" the streamline toward the equator in the magnetic regime, and hence, if the streamline does become potentially equator crossing, will increase the compression ratio $\mathscr{C}$ of the WCD.

Fig. 5 shows the streamlines computed with magnetic fields of B = 10, 30 and 60G. As can be seen the effect is dramatic. The IR continuum emission is also shown in Fig. 5 along with that calculated from an equivalent non-magnetic model. It is clear from these figures that the effect of magnetic fields can be enough to increase the continuum emission to such an extent that it *may* account for the total observed emission although the spectral shape of the excess is not matched exactly. However, given the approximate fashion in which the calculation has been attempted, it is fair to conclude that in principle, enough emission may be produced by this magnetic model.

5. Discussion

From the results presented above, it has been clearly shown that the simple additions to the standard WCD model will not enable the model to account for observed discs. The introduction of a magnetic field is a major qualitative change to the WCD model, which may enable it to account for the observed continuum emission. It is possible that several effects may be acting simultaneously, but this would require a much more "finely tuned" star than is required by introducing a magnetic field.

Is the proposition of a magnetically generated WCD a reasonable one? How may such fields be generated? What other facets of Be star observations could this explain?

The convective cores of massive stars may produce a magnetic field, although this field should then be present in both B and Be stars, thereby *not* separating the two classes of star by rotational velocity as observed. The rotation of stars generates meridional circulation currents within the star (Mestel 1953, Sweet 1950, Eddington 1925, Vogt 1925) arising from conservation of energy on equipotentials. The velocities calculated from models are low within the star (typically less than 0.1cm s^{-1} Tassoul & Tassoul 1982), but increase toward the surface inversely proportionally to the density. Zahn (1992) also points out that a star with a strong wind may induce further meridional motion, through angular momentum transport. However, as the surface is essentially at rest then a turbulent layer dissipates the kinetic energy below the photosphere (see eg. Urpin et al. 1996, Tassoul & Tassoul 1982). These studies of rotating stars, however, neglect the effects of magnetic fields within the star. Massive stars also possess atmospheric convection zones. It may be possible that the outer turbulent/convective layer is a site for a supplemental magnetic field to be generated. If so then this may point to a rotationally induced/supplemented magnetic field being the difference between B and Be stars, hence again establishing a rotational difference between B and Be stars.

Magnetic fields supplemented in this way may also promote the phase changes seen to occur in B stars (B $\leftrightarrow$ Be, Be $\leftrightarrow$ Be-shell). This change has perplexed researchers working in this area; if the disc is produced as a direct result of rotation alone then its apparent disappearance would logically imply that the rotation velocity of a star changes! Clearly this is incorrect, but a realignment of a rotationally produced magnetic field (or indeed it becoming chaotic with much small scale structure) is much easier to rationalize. Of course this *is* speculation, and a magnetic field supplemented in such a thin layer is unlikely to have such a simple dipole structure as has been assumed here, and therefore the results presented above must still only be a guide.

As yet no attempt has been made to assess the global or local stability of the disc. Should the disc become unstable to local perturbations, it will become turbulent. The net effect of this will be to increase the effective local sound-speed in the disc ie. $a_d \rightarrow (a_d^2 + a_t^2)^{1/2}$, where a_t is the turbulent velocity. This extra turbulent energy will then force the disc to expand. The net effect of perturbations growing whilst they are advected radially outwards is that the turbulent velocity a_t will grow with radius, forcing the disc to flare at radii where a_t becomes appreciable compared to the local sound speed in the disc a_d (refer to Eq. 7). This will cause the density to drop off faster with radius in the outer parts of the disc than in the inner parts as the mass flux in the disc does not change significantly (see Sect. 2). Hence the density power law derived from radio observations, probing the

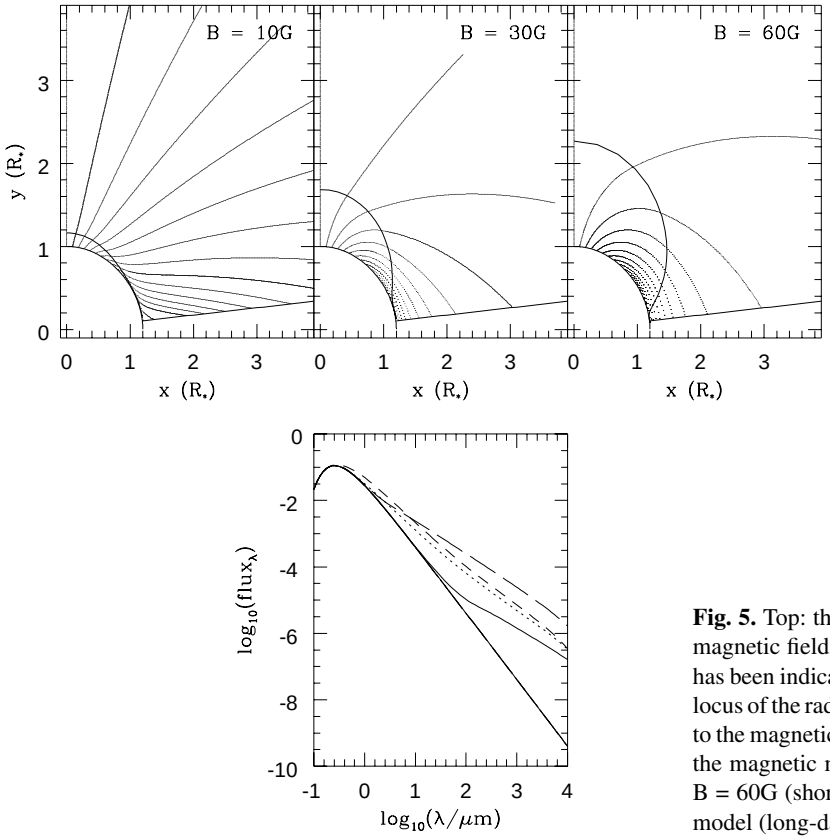

Fig. 5. Top: the streamlines calculated from the model with a dipolar magnetic field of B = 10G, 30G, and 60G (see text). The disc surface has been indicated (the disc has an opening angle of $\theta = 5^\circ$), as has the locus of the radii at which the kinetic energy density in the wins is equal to the magnetic energy density. Bottom: the IR continuum emission for the magnetic models with B=10G (solid line), B= 30G (dotted line), B = 60G (short-dashed line), and also for the standard unmagnetised model (long-dashed line).

outer disc, should be steeper than that derived from IR observations, which is just the effect that is observed (Dougherty et al. 1991, Taylor et al. 1990). This suggestion is given strength by similar simulations and stability analyses peformed by Stevens et al. (1992) in their colliding winds model for early type binaries, and also by Vishniac (1994) who considered the stability of a shock-bounded slab of gas. Both of these investigations did show that the shock-bounded region is unstable. As a simple explanation of the differing density power laws from the IR and radio observations, it is felt that stability analyses should be extended to WCDs to reconcile the observations.

6. Conclusion

A discussion of the IR continuum emission from WCDs has been presented. It is confirmed that the basic WCD model can not produce the IR emission observed from "real" Be star discs. Without invoking a serious asymmetry in the mass loss rate (which, in the limit will essentially lead to the standard disc model of Poeckert & Marlborough 1978, or Waters 1986), a possible addendum considered here to the standard model of Bjorkman & Cassinelli is that generated from a magnetic field with a strength of tens of gauss. Until reliable measurements of Be star magnetic fields are obtained, this hypothesis shall remain exactly that. However, it is now clear that by itself the WCD model is insufficient to explain observed discs.

Acknowledgements. I thank H.M. LLoyd for reading and suggesting improvements to the first draft of this paper, and also the referee, J.M. Marlborough, for constructive comments and criticism.

References

Ando H., 1986, A&A, 163, 97
de Araùjo F. X., de Freitas Pacheco J. A., 1989, MNRAS, 241, 543
Barker P.K., Landstreet J.D., Marlborough J.D., Thompson, I., Maza, J., 1981, ApJ, 250, 300
Bjorkman J.E., Cassinelli J.P., 1993, ApJ, 409, 429
Castor J.I., Abbott D.C., Klein R.I., 1975, ApJ, 195, 157
Dougherty S.M., Taylor A.R., Clark T.A., 1991, AJ, 102, 1753
Eddington A.S., 1925, Observatory, 48, 73
Fox G.K., 1993, MNRAS, 260, 525
Friend D.B., Abbott D.C., 1986, ApJ, 311, 701
Friend D.B., MacGregor K.B., 1984, ApJ, 282, 591
Hanuschik R.W., 1996, A&A, 308, 170
Kastner J.H., Mazzali P.A., 1989, A&A, 210, 295
Kudritzki R.P., Pauldrach A., Puls J., Abbott D. C., 1989, A&A, 219, 205
Landstreet J.D., 1982, ApJ, 258, 639
Lucy L.B., Solomon P.M., 1970, AJ, 159, 879
MacGregor K.B., Hartmann L., Raymond J.C., 1979, ApJ, 231, 514
Mestel L., 1953, MNRAS, 113, 716
Nerney S., 1980, ApJ, 242, 723
Owocki S.P., Castor J.I., Rybicki G.B., 1988, ApJ, 335, 914
Owocki S.P., Cranmer S.R., Blondin J.M., 1994, ApJ, 424, 887
Owocki S.P., Rybicki G.B., 1984, ApJ, 284, 337
Poe C.H., Friend D.B., 1986, ApJ, 311, 317

Poeckert R., Marlborough J.M., 1978, ApJ, 220, 940
Porter J.M., 1996, MNRAS, 280, L31
Porter J.M., Drew J.E., 1995, A&A, 296, 761
Quirrenbach A., Buscher D.F., Mozurkewich D., Hummel C.A., Armstrong J.T., A&A, 283, L13
Slettebak A., 1979, Sp. Sci. Rev., 23, 541
Springmann U.W.E., Pauldrach A.W.A., 1992, A&A, 262, 515
Stevens I.R., Blondin J.M., Pollock A.M.T., 1992, ApJ, 386, 265
Sweet P.A., 1950, MNRAS, 110, 548
Tassoul J.-L., Tassoul M., 1982, ApJs, 49, 317
Taylor A.R., Waters L.B.F.M., Bjorkman K.S., Dougherty S.M., 1990, A&A 231, 453
Urpin V.A., Shalybkov D.A., Spruit H.C., 1996, A&A, 306, 455
Vishniac E.T., 1994, ApJ, 428, 186
Vogt H., 1925, Astr. Nach., 223, 229
Waters L.B.F.M., 1986, A&A, 162, 121
Waters L.B.F.M., Cotè J., Lamers H.J.G.L.M., 1987,A&A, 185, 206
Waters L.B.F.M., Marlborough J.M., 1992, A&A 253, L25
Willson L.A., 1986, PASP, 98, 370
Zaal P.A., Waters L.B.F.M., Marlborough J.M., 1995, A&A, 299, 574
Zahn J.-P., 1992, A&A, 265, 115

This article was processed by the author using Springer-Verlag LaTeX A&A style file *L-AA* version 3.